MJSAT

Malaysian Journal of Science and Advanced Technology

journal homepage: https://mjsat.com.my/

Influence of Injection Timing on Combustion Characteristics, Performance, and Emission Behaviour of Dual-Fuel Engines

Abdullah Al Rifat, Md. Arafat Rahman*[1], and Md. Mizanur Rahman[1]

[1]*Department of Mechanical Engineering, Chittagong University of Engineering and Technology, Chittagong, Bangladesh.*

KEYWORDS

Injection Timing
Dual Fuel
Combustion
Performance
Emission

ARTICLE HISTORY

Received 23 November 2025
Received in revised form 24 May 2026
Accepted 7 June 2026
Available online 21 June 2026

ABSTRACT

At low loads, dual-fuel engines typically exhibit lower thermal efficiency and higher emissions. In this study, Ansys Forte 2023 R1 was used to model the combustion, performance, and emission characteristics of a methane-diesel dual-fuel engine at injection timings (IT) of 3°, 5°, 7°, and 9° bTDC under a 0.44 MPa load. The CFD simulation employed a modified re-entrant bowl piston with a 50% methane energy share and a 110° spray angle, where methane was premixed through intake manifold injection. Results show that maximum cylinder pressure, temperature, and apparent heat release rate increase with advancing IT. The highest thermal efficiency (34.11 %) and lowest indicated specific fuel consumption were observed at 7° bTDC. O and OH radical formation rose when shifting IT from 3° to 9° bTDC due to improved mixing, which also enhanced premixed combustion. Therefore, CO, UHC, VOC, and soot emissions decreased as IT advanced. However, earlier injection produced higher peak temperatures, leading to increased NOx formation compared to later IT. However, 7° bTDC was identified as the optimal injection timing, providing the best balance of combustion efficiency, engine performance, and acceptable emission levels.

1. INTRODUCTION

ThisThe formation of the pollutants has been the focus of concern for environmental concerns during the past decades. The emissions from human activities and natural sources have substantial risk to nature and human health. Increasing the volume percentage of these emissions results in a serious problem in both developed and developing countries. A significant amount of emissions is coming out from the internal combustion engine (ICE). ICEs have emerged significantly on account of their bowl-shaped design with enhanced performance and lowered emission percentage. Computational fluid dynamics (CFD) investigation plays a crucial role in optimizing engine performance and acceptable emissions. CFD numerical modelling reduces cost and achieves quick analysis to make decisions.

Modern diesel engines have heavy-duty applications due to dual fuel adaptability and high thermal efficiency [1]. Controlling injection parameters is crucial for optimum performance, combustion, and emissions [2]. Ignition delay, efficiency, and performance are influenced by the fuel injection timing (IT) [3]. The effect of IT has been extensively investigated in diesel engines through both experiments and simulations. Summarizes, IT controls the ignition delay and premixed fraction [2], [4], [5]. Earlier fuel injection during compression gives higher ignition delay and allows more time for fuel-air mixing before the beginning of combustion, resulting in peak cylinder pressure and temperature during the burning of fuel [6]. Fuel injection is a critical phenomenon receiving significant attention from researchers and designers. Spray tip modification, number of nozzles, nozzle diameter, and geometry of the nozzle holes are considered important fuel injection parameters [7].

Researchers are now currently focusing on the combustion chamber design and then doing CFD simulation in a dual-fuel engine to see the effect of combustion, performance, and emission parameters. For improving the fuel injection system, both the amount of fuel and IT can be optimized with engine speed and load [8]. Uniform and quick mixing of intake charge with fuel and appropriate control of fuel spray is crucial for optimum performance and emissions [9]. Optimum IT plays a significant role in ICEs fueled with various fuels and fuel blends [10]. The modifications in the injection system and timing resulted in a change in flow pattern and affected in-cylinder conditions [11]. However, concentrating on the fuel

*Corresponding author:
E-mail address: Md. Arafat Rahman < arafat@cuet.ac.bd >.
https://doi.org/10.56532/mjsat.v6i2.661
2785-8901/

injection parameters and optimizing these parameters can significantly improve performance and reduce emissions. The combustion, performance, and emission parameters are modified by changing the injection parameters [12]–[14].

Shi et. al. [15] investigated multi-optimization of injection parameters that influence emission. They reported that there is a clear trade-off between soot and nitrogen oxide (NO_X) emissions. A study of the emission characteristics of Fischer-Tropsch fuel in diesel engines suggests that injection timing, pressure, and amount are significant factors in optimizing soot and NO_X emissions. Sun et al. [16] investigated injection characteristics in a diesel engine. They reported that by delaying the pilot injection timing, the peak cylinder pressure (PCP), coupled cetane number (CN), and thermal efficiency rise, while the brake specific fuel consumption (BSFC) declines, carbon mono-oxide (CO) and hydrocarbon (HC) emissions rise, and NO_X emissions reduce. The number of particles increased and subsequently decreased as particle size increased, with a peak in the 25-35 nm range. Usman et al. [17] investigated fuel injection attribute optimization using the response surface approach. They found that increasing the nozzle protrusion from 1.5 mm to 2.5 mm increased NO_X emissions by 2.18% and 7.83%, respectively. Furthermore, at 230 bar pressures, increasing the protrusion from 1.5 to 2.5 mm increased HC emissions by 2.86%. Whereas at 240 bar pressure, HC emission reduced by 4.23%.

Mei et al. [18] investigated the effect of two pilot injections in a diesel engine at 0.44 MPa low load using experiment and simulation. Delaying the first pilot injection (SOI-P1) or advancing the second pilot injection (SOI-P2) resulted in higher pressure, heat release rate (HRR), and temperature peak. Throughout the two pilot injection times, SOI-P2 mostly determined ignition time, while SOI-P1 influenced the first released heat peak. Delays in SOI−P1 or advances in SOI−P2 led to considerable increases in NO_X generation, while soot formation varied slightly. Ahmed et al. [5] studied the effect of injection timing on a CI engine fueled by butanol diesel. The GT-Power numerical simulation package was used to simulate four injection timings) and two brake mean effective pressure loads of 4.5 bar and 10.5 bar at a constant engine speed of 1800 rpm. Retarded injection time, 10◦CA bTDC, led to optimal performance, combustion, and emissions. Fuel 15B performed well in terms of brake thermal efficiency (BTE), increased HRR, and reduced the emissions of HC, CO, and NO_X. Zhou et al. [19] investigated the IT effect on a dual-fuel engine with low and medium loads. Setting the diesel injection timing to 27° crank angle (CA) bTDC under medium-speed low-load conditions and a 40% natural gas (NG) substitution rate increased engine output power by 9.03%, reduced BSFC by 13.33%, and significantly lowered CO, CO_2, and HC emissions. Setting the diesel injection time to 25°CA bTDC at medium-speed, medium-load scenarios with an 80% NG replacement rate boosted engine output power by 14.62%, lowered BSFC by 11.73%, and considerably decreased CO, CO_2, and HC emissions.

The purpose of this research is to assess the performance, combustion, and emission results of a dual-fuel diesel engine by altering injection timing with ANSYS Forte 2023 R1 CFD modeling software. While injection timing has a substantial impact on air-fuel mixing, ignition delay, and combustion characteristics in diesel engines, it has received little attention in studies of methane-diesel dual-fuel combustion. This work conducts a complete CFD-based investigation of various diesel injection timings to disclose their effects on in-cylinder pressure, thermal efficiency, fuel consumption, and emission production mechanisms. The findings support injection timing modification as a viable method for enhancing performance and lowering emissions in dual-fuel engines.

2. NUMERICAL MODELLING

To provide for the combustion chamber's symmetry, the modified re-entrant piston bowl in Figure 1 with eight injectors is split into one-eighth segments. The modified re-entrant bowl has a narrow lip, which increases squish and swirl as the piston approaches the top. This design generates high-velocity vortices and higher turbulent kinetic energy, which speeds up fuel vaporization and mixing. It greatly improves the premixed phase by promoting a more consistent and homogenous air-fuel mixture as well as greater heat dispersion. This results in faster, more steady combustion, higher thermal efficiency, and lower emissions than traditional cylindrical or open-style bowl designs. [20]–[22]. For injectors with periodic spacing, parameters like injection pressure, temperature, air-fuel mixing, and combustion activities are assumed to be identical throughout each hole in the injector and their associated spray [23]. In this investigation, the sector angle is fixed to 45°, and periodic boundary conditions are added to the periodic faces.

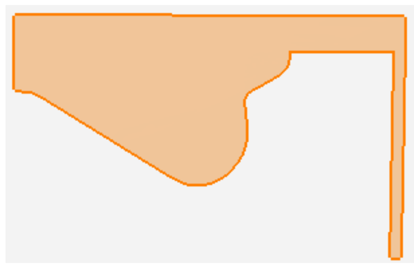

Fig. 1. Modified re-entrant bowl.

The peak cylinder pressure (PCP) for the modified re-entrant bowl shape ranges from 7.75 MPa to 8.23 MPa for mesh counts of 16000, 18120, and 21735, as shown in Figure 2. Mesh counts of 18120 and 21735 provide the higher PCP with 0.73% variation. Mesh count 18120 has the PCP of 8.23 MPa and is used as the final mesh for the numerical analysis.

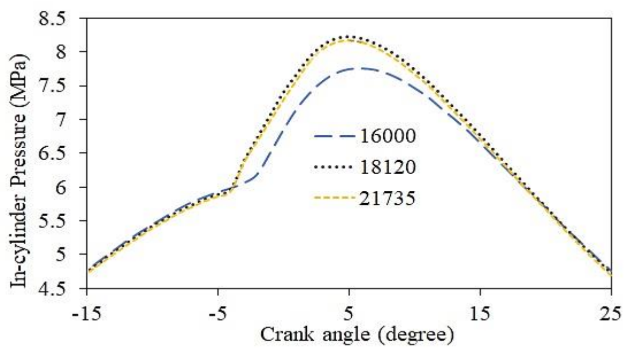

Fig. 2. Mesh independency study

Hydrocarbon (HC) and CO initially increased and subsequently reduced with methane energy share (MES), with a maximum drop of 35% in NOx at a 50% MES level [24]. CO levels dropped as the MES rose from 0 to 50%. CO emissions increased dramatically as the MES gets to 75%. Methane replaces a significant amount of oxygen within the intake manifold, reducing CO oxidation. At 75% MES, the diesel volume is exceedingly low to ensure total methane combustion and cannot burn on its own due to the higher auto-ignition temperature. Incomplete combustion leads to greater CO emissions [25]. This study uses 50% MES to investigate combustion, performance, and emissions. The engine parameters for the modified re-entrant bowl are shown in Table 1.

Table 1. Engine parameters

Type of engine	Single cylinder, 4-stroke
Diameter×Stroke	13.97 cm×15.24 cm
Squish	0.56 cm
Connecting rod length	30.48 cm
Crevice width× height	0.167 cm× 3.72621 cm
Geometric compression ratio	11.1957
No. of nozzle	8
Nozzle orifice radius	0.009805 cm
Speed	1200 rpm
Start of pilot fuel injection	3°, 5°, 7° and 9° bTDC
Spray angle	110°
Inflow droplet temperature	111°C
Discharge co-efficient	0.7

Rifat et al. studied the spray angle (SA) effects on methane diesel dual fuel engine. Five different spray angles of 100°, 105°, 110°, 115°, and 120° were analyzed for combustion, performance and emissions with 50% methane energy share under 0.44 MPa load. The optimum spray angle was obtained at 110° [26]. Smaller squish clearance gives improved combustion and the limitation for keeping too small clearance like higher NO_X, excessive heat transfer loss, risk of piston heating head etc. Also, higher squish clearance can change combustion phasing and stability [27], [28]. The interaction of wide SA of 110° and small squish clearance 0.56 cm, creates high turbulence and fast mixing but it needs to be matched with injection timing and bowl geometry for lowering wall wetting. For better combustion, squish needs to be optimized. For setting the chemical reaction mechanism, a Chemkin file was generated by merging the diesel and methane Chemkin mechanism file with CHEMKIN 2023 R1. The n-heptane [32] mechanism describes how the diesel fuel combusts in a diesel engine. The GRI-Mech 3.0 [33], is the chemical kinetics mechanism for modeling of methane combustion. The total species and reaction numbers were lower than the individual sum of the two mechanisms' species and reaction numbers. The reason is that both mechanisms contain the similar species and reactions. The generated Chemkin file is then chosen for the chemistry set under the chemistry model. Some of the other CFD sub-models are RNG k-ϵ for turbulence, KH-RT for the breakup model, the Han-Reitz model for heat transfer, the two-step semi-empirical model for soot, and the Zeldovich mechanism for NO_X, which are used for analysis. Table 2 reports the initial and boundary conditions parameters associated data for the analysis.

Table 2. Boundary and initial conditions

Parameters	Associated data
Intake valve closing	165° bTDC
Exhaust valve opening	125° aTDC
Intake pressure	0.233 MPa
Intake charge temperature	111°C
Primary swirl ratio	0.5
Primary swirl shape factor	3.11
Turbulent kinetic energy	1 m^2/sec^2
Piston wall temperature	127°C
Head temperature	102°C
Liner temperature	92°C

The simulated PCP for diesel combustion is validated with the Musculus experimental data [29] as in Figure 3. There is close observation between the numerical and experimental results with a variation of approximately 2.46%. In simulation, ± 5% deviations are normally considered acceptable for model validation [30]. This 2.46% PCP deviation represents the model is capable of precisely capturing the in-cylinder pressure variation under the same operating conditions and the engine geometry data.

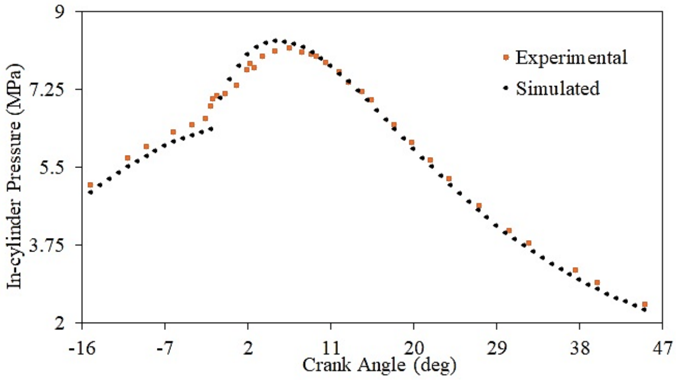

Fig. 3. Validation for cylinder pressure with Musculus [29]

3. Results and Discussion

Simulated cylinder pressure (CP) and mean cylinder temperature (CT) with crank angle are shown in Figure 4 and Figure 5, respectively, for different injection timing (IT). Advancing IT results in an early start of combustion, so CP and heat release rate (HRR) rise when the piston still moves towards top dead center (TDC). Retarding IT results in CP and HRR rising when the piston starts to descend. Advanced IT has more time for premixed burn and thus work done, and peak cylinder pressure (PCP) is higher as IT shifts from 3° to 9° bTDC. The temperature distribution also has the same trend.

The apparent heat release rate (AHRR) plotted with crank angle is shown in Figure 6. Advanced IT shifts the AHHR curve earlier in the combustion cycle. Earlier injection results in the release of higher heat sooner and reaches peak AHRR earlier. The peak AHRR for 9°, 7°, 5°, and 3° bTDC IT are 533, 522.2, 467, and 365 J/deg, respectively, and the AHRR curve shifts right from 9° to 3° bTDC IT. Thus, the advanced IT implies more rapid and intense combustion.

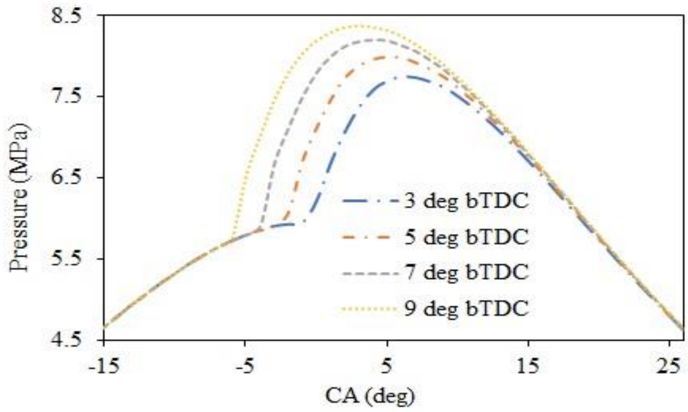

Fig. 4. In-cylinder pressure variation with crank angle under different injection timing

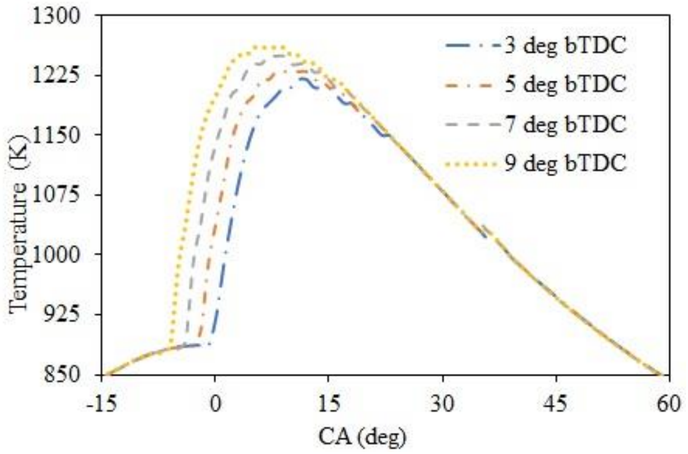

Fig. 5. In-cylinder temperature variation with crank angle under different injection timing

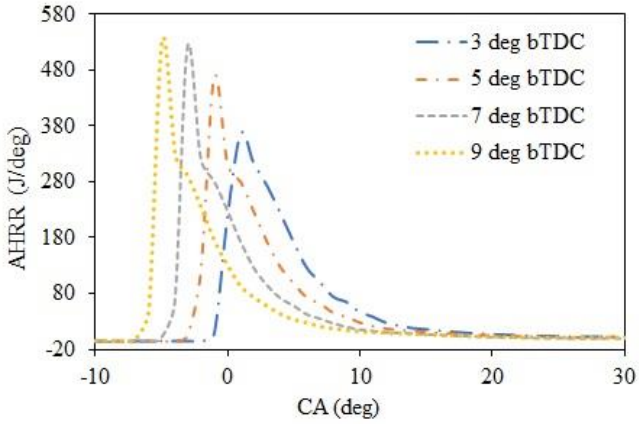

Fig. 6. AHRR variation with crank angle under different injection timing

The total apparent heat release (AHR) demonstrates how much chemical energy is utilized in the cylinder and shows the total contribution of both diesel and methane oxidation. The AHR is higher for the 7° bTDC as shown in Figure 7(a). Peak AHRR represents how fast fuel burns at a certain CA. At 9° bTDC IT, as for early injection, more time for premixing and subjects to more rapid combustion results in peak sharp AHRR. The total AHRR relay on the amount of fuel combust effectively over the cycle. The highest total AHRR at 7° bTDC indicates better thermodynamic efficiency by balancing premixed and diffusion combustion [1], [31]. Methane oxidation is slower and needs O and OH radicals from the diesel flame. Methane oxidation strongly occurred by the O and OH radical. The OH radical has an important role in initiating methane breakdown. The O radical directly contributed in the methane breakdown and generating additional OH radicals and thereby accelerates the reaction [32]–[34]. Early IT has more time to interact with the methane-air premixed charge as the piston is still moving towards TDC and a higher amount of methane is burnt. So, combustion efficiency increases from 3° to 9° bTDC as shown in Figure 7(b).

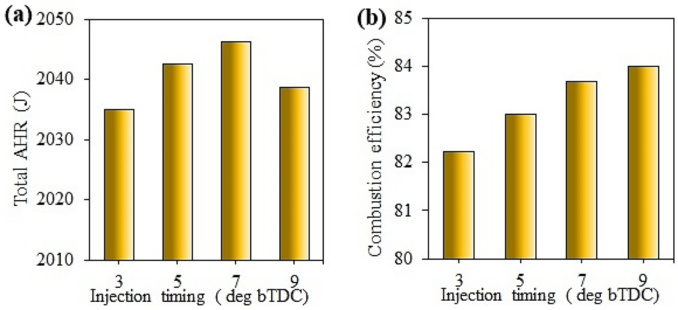

Fig. 7. Combustion attributes, (a) Total AHR, and (b) Combustion efficiency

Indicated specific fuel consumption (ISFC) demonstrates the amount of fuel needed per unit of indicated power. Lower ISFC is for more efficient fuel utilization. The ISFC for different IT are shown in Figure 8 (a). 7° bTDC has the lower ISFC because of stronger premixing and better combustion. The area under the pressure-crank angle curve gives the indicated work. Figure 8 (b) shows the thermal efficiency for different IT, and it is maximum for 7° bTDC IT. A higher amount of heat was released before TDC at 9° bTDC. For early heat release pressure rises much during compression compared with 7° bTDC IT that resists piston motion. A certain amount of AHR is used to overcome the resistive motion and thus net work output reduces compared with 7° bTDC [35].Thermal efficiency is how effectively combustion energy is converted into work. Late IT means more of the heat release occurs as the piston starts moving and descends from TDC, resulting in less useful work and heat loss through walls and exhaust. 7° bTDC gives the lowest ISFC and highest thermal efficiency, signifying better fuel utilization, more complete combustion, and lower heat loss.

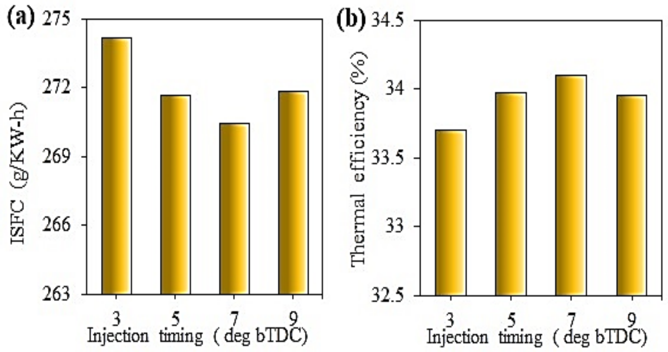

Fig. 8. Performance attributes, (a) ISFC, and (b) Thermal efficiency

The NO_X emission significantly increases from 3° bTDC IT by 8.27%, 16.54%, and 26.69% for 5°, 7°, and 9° bTDC, respectively, as shown in Figure 9(a). Higher PCP and PCT for early injection give more time for NO_X formation and available oxygen at high temperature. The soot emission trend is seen opposite to the NO_X emission shown in Figure 9(c). Advancing IT promotes more complete combustion in the high-temperature region and more time to mix with air, thus reducing fuel-rich pockets that produce soot. NO_X formation occurs for high temperature lean mixture, conversely soot formation by low temperature rich mixture. The opposite trend of NO_X, and soot is the conventional NO_X-soot trade off [36]. Advancing IT from 3° bTDC towards 9° bTDC, NO_X emission increases but soot emission decreases, and there is an opposite trend for NO_X and soot that demonstrates conventional NO_X-soot trade-off.

CO emission is the intermediate product formed during combustion in the fuel-rich region where carbon cannot fully oxidize to CO_2 formation. The CO emission is 3.27%, 5.61%, and 7.48% lower in 5°, 7°, and 9° bTDC IT compared with 3° bTDC IT, as shown in Figure 9(a). The oxidation of CO to CO_2 is due to the reaction of CO with O and OH radicals. Advancing the IT with PCT increases the rate of free radical formation. Figures 10(a) and 10(b) show the O and OH free radical formation in mole fraction with crank angle with different IT. The total amount of O radical formation is 6.41%, 14.3%, and 25.2% higher for 5°, 7°, and 9° bTDC IT, respectively, and OH radical formation is 5.2%, 11.51%, and 20.68% higher, respectively, compared with 3° bTDC IT. Thus, it signifies the CO emission decreases because of higher radical formation with increasing IT.

Late IT has very limited premixing, diesel combusts rapidly, radical formation is lower, and there is poor mixing of methane-air with diesel. Thus, large unburned pockets of methane resulted in higher amounts of UHC and VOC emissions. The amount of UHC emission for 3° bTDC IT is 48.7 g/kW-h and decreases with increases in IT as shown in Figure 9(b). UHC is the total amount of unoxidized diesel-methane fuel during combustion. Some amount of fuel is partially oxidized into intermediates like aldehyde, ketone, and short-chain hydrocarbons. The UHC and partially oxidized fuels are collectively classified as VOC. The amount of VOC emission is 3.56%, 7.51%, and 8.70% lower in IT 5°, 7°, and 9° bTDC, respectively, compared with 3° bTDC IT as shown in Figure 9(b). Table 3 shows the comparative performance and emission for the IT effect compared with 7° bTDC IT, and the recommendation from this investigation is 7° bTDC IT, which gives the best performance and emission control.

Table 3. Normalized engine performance and emission for injection timing effect compared with 7 ° bTDC IT

Injection Timing (bTDC)	3°	5°	7°	9°
ISFC	1.39% ↑	0.45% ↑	-	0.52% ↑
Total AHR	0.55% ↓	0.19% ↓	-	0.37% ↓
Thermal Efficiency	1.20% ↓	0.40% ↓	-	0.47% ↓
NO_X	14.19% ↓	7.10% ↓	-	8.71% ↑
Soot	46.77% ↑	19.69% ↑	-	18.77%↓
CO	5.94% ↑	2.48% ↑	-	1.98% ↓
UHC	7.74% ↑	3.54% ↑	-	0.88% ↓
VOC	8.12% ↑	3.63% ↑	-	1.28% ↓

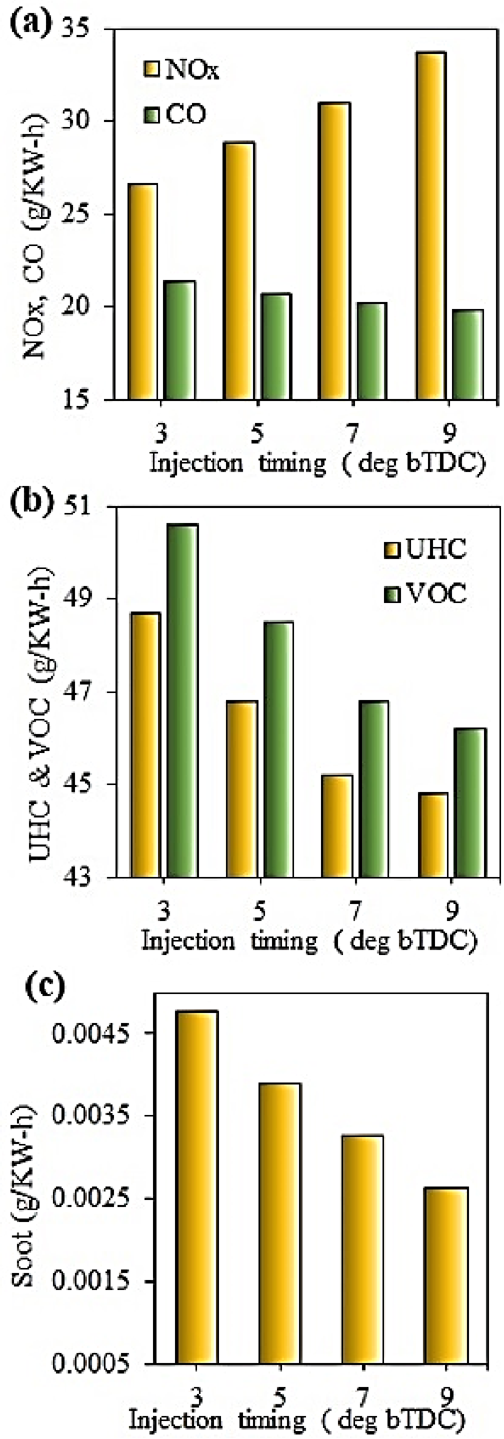

Fig. 9. Emission attributes, (a) NO_X and CO, (b) UHC and VOC, and (c) Soot

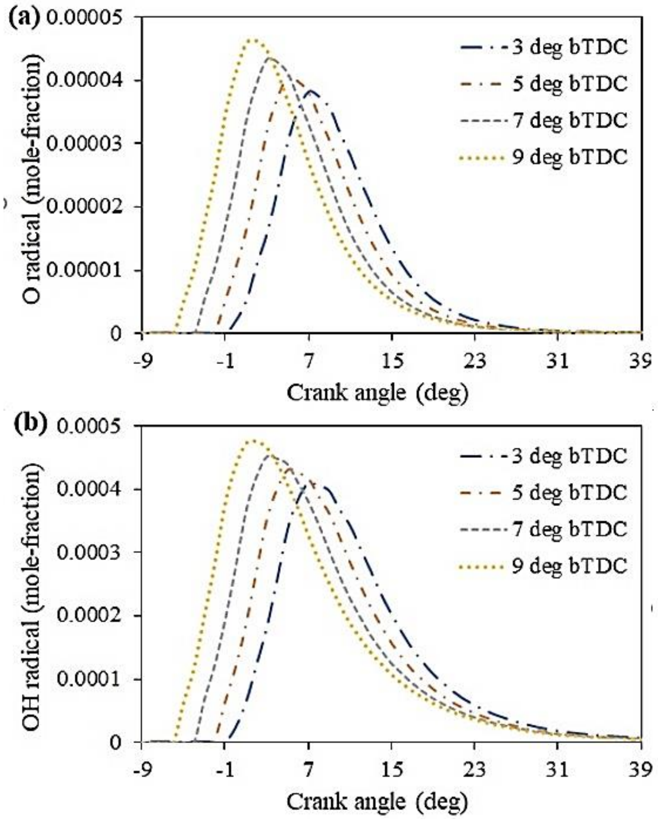

Fig. 10. (a) O radicals, and (b) OH radical's formation with crank angle

The consistent identification of 7° bTDC as the optimum injection timing across combustion, performance, and emission metrics has practical significance for dual-fuel engine calibration. Because ignition delay and premixed burn fraction respond continuously to injection timing rather than switching abruptly at a single crank angle, the narrow band around 7° bTDC identified here is consistent with the general injection-timing sensitivity reported for common-rail diesel and dual-fuel systems elsewhere [2], [3], [10]. Modern electronically controlled common-rail injection systems can adjust injection timing in fine increments across the engine map, so the 7° bTDC set point identified in this 50% MES, 1200 rpm case could, in principle, serve as a calibration target for similar dual-fuel configurations operating near this load and speed. However, because the optimum shifts with methane energy share and operating condition [19], [24], any field implementation would require a timing map that adapts IT to MES and load rather than a single fixed setting.

These trends also complement earlier findings on combustion chamber geometry effects in dual-fuel engines. The modified re-entrant bowl used here, which enhances squish and swirl relative to conventional cylindrical or open bowls [20]–[22], appears to work synergistically with advanced injection timing: both promote more complete premixing ahead of the diffusion-controlled phase of combustion, and both were shown, individually, to raise thermal efficiency while suppressing soot and unburned hydrocarbon emissions. This suggests that injection timing optimization and piston bowl design should not be treated as independent variables in dual-fuel engine development, but rather co-optimized together, consistent with the coupled effect of injection parameters and chamber geometry reported for conventional diesel combustion [7], [27], [28].

Several simplifications in this study should be acknowledged when interpreting the results. The combustion chamber was represented as a 45° periodic sector rather than the full engine geometry, which assumes identical spray and combustion behaviour across all eight injector holes and cannot capture hole-to-hole or cycle-to-cycle asymmetries that may exist in a real engine. The chemical kinetics were modelled by merging an n-heptane mechanism for diesel with GRI-Mech 3.0 for methane [32], [33], together with a two-step semi-empirical soot model and the Zeldovich mechanism for NOX; while computationally efficient, these reduced-order sub-models trade some predictive accuracy for tractable simulation time relative to detailed multi-component surrogate fuel chemistry. Model validation was limited to a single operating point against Musculus's diesel-only PCP data [29], with a 2.46% deviation; a broader validation across multiple loads, speeds, and dual-fuel operating points would strengthen confidence in the absolute emission values, even though the relative trends across injection timings are expected to be robust. Finally, all cases were simulated at a fixed 50% MES and 1200 rpm, so the interaction between IT, MES, and load was not explored here.

Building on these findings, future work should extend the present CFD framework to a wider matrix of MES levels, engine speeds, and loads to establish a generalized IT-MES calibration map, and should incorporate the modified re-entrant bowl geometry into transient, multi-cycle simulations to assess cycle-to-cycle variability. Coupling the numerical predictions with dedicated experimental testing on a dual-fuel research engine equipped with in-cylinder pressure and exhaust emission instrumentation would allow direct validation of the NOX-soot trade-off and radical formation trends reported here, and would help translate the 7° bTDC recommendation into a field-deployable injection timing strategy.

4. CONCLUSION

This numerical investigation examines how a dual-fuel (DF) engine with a modified re-entrant bowl at 50% MES is affected by injection timing (IT) in terms of combustion, emissions, and performance. The piston bowl was modeled as a 45° sector with eight injectors under periodic boundary conditions to save computational costs. Ansys Forte 2023 R1 was used to perform computational fluid dynamics (CFD) simulations for IT of 3°, 5°, 7°, and 9° bTDC. There are few observations that have been found in this investigation as follows:

a) The peak cylinder pressure (PCP), peak cylinder temperature (PCT), and apparent heat release rate (AHRR) were increased, and their associated curves shifted left with increasing IT. Total AHRR was found higher in 7° bTDC IT.
b) Thermal efficiency was found to be higher, about 34.11%, in 7° bTDC IT with the lowest indicated specific fuel consumption (ISFC) of 270.43 g/KW-h.
c) At 7° bTDC IT, the NO_X emissions peaked but were lower than at 9° bTDC IT. CO, UHC, VOC, and soot emissions are considerably lower for 7° bTDC IT in comparison with late injection.

Low load of dual-fuel engine has the higher emission percentages. The UHC, VOC, and CO are the lowest at 9° bTDC by 0.88%, 1.28%, and 1.98%, respectively, compared with 7° bTDC, but in terms of NO_X, 9° bTDC gives the higher percentage, about 8.71%. Compared with these two, 7° bTDC has the cumulatively lower amount of emissions. The IT of 5°, 7°, and 9° bTDC gives the best performance in terms of ISFC and thermal efficiency, as their values are close, but 7° gives the best performance. Despite increased NO_X emissions, 7° bTDC was found to be the most efficient configuration based on the overall trade-off between emissions and performance.

ACKNOWLEDGEMENTS

This work is financially supported by Chittagong University of Engineering & Technology (CUET), Bangladesh through research grant no. CUET/CHSR-47-47.4.11. The corresponding author is responsible for ensuring that the descriptions are accurate and agreed by all authors.

REFERENCES

[1] J. B. Heywood, Internal combustion engine fundamentals. McGraw-Hill Education, 2018.

[2] H.-M. Baek, G.-S. Jung, Q. D. Vuong, J.-U. Lee, and J.-W. Lee, "Effect of performance by excessive advanced fuel injection timing on marine diesel engine," Appl. Sci., vol. 13, no. 16, p. 9263, 2023, doi: https://doi.org/10.3390/app13169263.

[3] J. Benajes, A. García, J. Monsalve-Serrano, and R. L. Sari, "Fuel consumption and engine-out emissions estimations of a light-duty engine running in dual-mode RCCI/CDC with different fuels and driving cycles," Energy, vol. 157, pp. 19–30, 2018, doi: https://doi.org/10.1016/j.energy.2018.05.144.

[4] J. Li et al., "Effects of different injection timing on the performance, combustion and emission characteristics of diesel/ethanol/n-butanol blended diesel engine based on multi-objective optimization theory," Energy, vol. 260, p. 125056, 2022, doi: https://doi.org/10.1016/j.energy.2022.125056.

[5] S. A. Ahmed, S. Zhou, Y. Zhu, Y. Feng, A. Malik, and N. Ahmad, "Influence of injection timing on performance and exhaust emission of CI engine fuelled with butanol-diesel using a 1D GT-power model," Processes, vol. 7, no. 5, p. 299, 2019, doi: https://doi.org/10.3390/pr7050299.

[6] T. Kamimoto and M. Bae, "High combustion temperature for the reduction of particulate in diesel engines," SAE Trans., pp. 692–701, 1988, doi: https://doi.org/10.4271/880423.

[7] P. J. Shayler and H. K. Ng, "Simulation studies of the effect of fuel injection pattern on NO and soot formation in diesel engines," SAE Technical Paper, 2004, doi: https://doi.org/10.4271/2004-01-0116.

[8] Y. Deng, H. Liu, X. Zhao, and J. Chen, "Effects of cold start control strategy on cold start performance of the diesel engine based on a comprehensive preheat diesel engine model," Appl. Energy, vol. 210, pp. 279–287, 2018, doi: https://doi.org/10.1016/j.apenergy.2017.10.093.

[9] M. H. M. Yasin et al., "Study of a diesel engine performance with exhaust gas recirculation (EGR) system fuelled with palm biodiesel," Energy Procedia, vol. 110, pp. 26–31, 2017.

[10] H. A. Dhahad, M. A. Fayad, M. T. Chaichan, A. A. Jaber, and T. Megaritis, "Influence of fuel injection timing strategies on performance, combustion, emissions and particulate matter characteristics fueled with rapeseed methyl ester in modern diesel engine," Fuel, vol. 306, p. 121589, 2021, doi: https://doi.org/10.1016/j.fuel.2021.121589.

[11] S. Talesh Amiri, R. Shafaghat, O. Jahanian, and A. H. Fakhari, "Numerical investigation of reactivity controlled compression ignition engine performance under fuel aggregation collision to piston bowl rim edge situation," Iran. J. Energy Environ., vol. 12, no. 1, pp. 10–17, 2021.

[12] S. S. Motallebi Hasankola, R. Shafaghat, O. Jahanian, and K. Nikzadfar, "An experimental investigation of the injection timing effect on the combustion phasing and emissions in reactivity-controlled compression ignition (RCCI) engine," J. Therm. Anal. Calorim., vol. 139, no. 4, pp. 2509–2516, 2020, doi: https://doi.org/10.1007/s10973-019-08761-0.

[13] A. H. Fakhari, R. Shafaghat, O. Jahanian, H. Ezoji, and S. S. Motallebi Hasankola, "Numerical simulation of natural gas/diesel dual-fuel engine for investigation of performance and emission," J. Therm. Anal. Calorim., vol. 139, no. 4, pp. 2455–2464, 2020, doi: https://doi.org/10.1007/s10973-019-08560-7.

[14] A. Ghaedi, R. Shafaghat, O. Jahanian, and S. S. Motallebi Hasankola, "Comparing the performance of a CI engine after replacing the mechanical injector with a common rail solenoid injector," J. Therm. Anal. Calorim., vol. 139, no. 4, pp. 2475–2485, 2020, doi: https://doi.org/10.1007/s10973-019-08760-1.

[15] J. Shi, K. Liu, M. Xu, and Z. Ji, "Multi-Optimization of Injection Parameters Affecting Emissions in a Diesel Engine Fueled with Fischer–Tropsch Fuel Based on NSGA-II," ACS omega, vol. 8, no. 23, pp. 20293–20302, 2023, doi: https://doi.org/10.1021/acsomega.2c07465.

[16] B. Sun, L. Zhang, S. Zhao, Q. Liu, F. Luo, and H. Wu, "Effect of cetane-coupled pilot injection parameters on diesel engine combustion and emissions," ACS omega, vol. 7, no. 50, pp. 46550–46563, 2022, doi: https://doi.org/10.1021/acsomega.2c05379.

[17] M. Usman et al., "Multipurpose optimization of fuel injection parameters for diesel engine using response surface methodology," Case Stud. Therm. Eng., vol. 52, p. 103718, 2023, doi: https://doi.org/10.1016/j.csite.2023.103718.

[18] D. Mei, Q. Yu, Z. Zhang, S. Yue, and L. Tu, "Effects of two pilot injection on combustion and emissions in a PCCI diesel engine," Energies, vol. 14, no. 6, p. 1651, 2021, doi: https://doi.org/10.3390/en14061651.

[19] H. Zhou, H.-W. Zhao, Y.-P. Huang, J.-H. Wei, and Y.-H. Peng, "Effects of injection timing on combustion and emission performance of dual-fuel diesel engine under low to medium load conditions," Energies, vol. 12, no. 12, p. 2349, 2019, doi: https://doi.org/10.3390/en12122349.

[20] A. Al Rifat, M. M. Rahman, and M. A. Rahman, "Effect of piston bowl geometry on combustion, performance, and emission characteristics of a dual-fuel engine," Futur. Energy, vol. 5, no. 1 SE-Articles, pp. 1–9, Oct. 2025, [Online]. Available:

[21] H. E. Gulcan and M. Ciniviz, "Experimental study on the effect of piston bowl geometry on the combustion performance and pollutant emissions of methane-diesel common rail dual-fuel engine," Fuel, vol. 345, p. 128175, 2023, doi: https://doi.org/10.1016/j.fuel.2023.128175.

[22] A.-H. Kakaee, A. Nasiri-Toosi, B. Partovi, and A. Paykani, "Effects of piston bowl geometry on combustion and emissions characteristics of a natural gas/diesel RCCI engine," Appl. Therm. Eng., vol. 102, pp. 1462–1472, 2016, doi: https://doi.org/10.1016/j.applthermaleng.2016.03.162.

[23] K. M. Rahman and Z. Ahmed, "Combustion and emission characteristics of a diesel engine operating with varying equivalence ratio and compression ratio-A CFD simulation," J. Eng. Adv., vol. 1, no. 03, pp. 101–110, 2020, doi: https://doi.org/10.38032/jea.2020.03.005.

[24] O. H. Ghazal, "Air pollution reduction and environment protection using methane fuel for turbocharged CI engines," J. Ecol. Eng., vol. 19, no. 5, pp. 52–58, 2018.

[25] G. Tripathi, P. Sharma, and A. Dhar, "Effect of methane augmentations on engine performance and emissions," Alexandria Eng. J., vol. 59, no. 1, pp. 429–439, 2020.

[26] A. Al Rifat, M. A. Rahman, M. M. Rahman, T. Hassan, and M. N. Haque, "Computational Analysis of Spray Angle Effects on Combustion and Emissions in Methane-Diesel Dual-Fuel Engine," Energy Sci. Eng., vol. 14, no. 3, pp. 1100–1112, 2026, doi: https://doi.org/10.1002/ese3.70427.

[27] Y. Kidoguchi, C. Yang, and K. Miwa, "Effect of high squish combustion chamber on simultaneous reduction of NOx and particulate from a direct-injection diesel engine," in International Fuels & Lubricants Meeting & Exposition, SAE Technical Paper, 1999, doi: https://doi.org/10.4271/1999-01-1502.

[28] V. S. Yaliwal, N. R. Banapurmath, N. M. Gireesh, R. S. Hosmath, T. Donateo, and P. G. Tewari, "Effect of nozzle and combustion chamber geometry on the performance of a diesel engine operated on dual fuel mode using renewable fuels," Renew. Energy, vol. 93, pp. 483–501,

2016.

[29] M. P. B. Musculus, "On the correlation between NOx emissions and the diesel premixed burn," SAE Trans., pp. 631–651, 2004, doi: https://doi.org/10.4271/2004-01-1401.

[30] F. Stern, R. Wilson, and J. Shao, "Quantitative V&V of CFD simulations and certification of CFD codes," Int. J. Numer. methods fluids, vol. 50, no. 11, pp. 1335–1355, 2006, doi: https://doi.org/10.1002/fld.1090.

[31] M. C. Cameretti, R. De Robbio, E. Mancaruso, and M. Palomba, "CFD study of dual fuel combustion in a research diesel engine fueled by hydrogen," Energies, vol. 15, no. 15, p. 5521, 2022, doi: https://doi.org/10.3390/en15155521.

[32] J. A. Miller and C. T. Bowman, "Mechanism and modeling of nitrogen chemistry in combustion," Prog. energy Combust. Sci., vol. 15, no. 4, pp. 287–338, 1989, doi: https://doi.org/10.1016/0360-1285(89)90017-8.

[33] W. Tsang and R. F. Hampson, "Chemical kinetic data base for combustion chemistry. Part I. Methane and related compounds," J. Phys. Chem. Ref. data, vol. 15, no. 3, pp. 1087–1279, 1986, doi: https://doi.org/10.1063/1.555759.

[34] C. K. Westbrook and F. L. Dryer, "Simplified reaction mechanisms for the oxidation of hydrocarbon fuels in flames," Combust. Sci. Technol., vol. 27, no. 1–2, pp. 31–43, 1981, doi: https://doi.org/10.1080/00102208108946970.

[35] S. Fygueroa, C. Villamar, and O. Fygueroa, "Thermodynamic study of the working cycle of a direct injection compression ignition engine," in Internal Combustion Engines, IntechOpen, 2012, doi: https://doi.org/10.5772/50028.

[36] H. Zhu, S. V Bohac, K. Nakashima, L. M. Hagen, Z. Huang, and D. N. Assanis, "Effect of fuel oxygen on the trade-offs between soot, NOx and combustion efficiency in premixed low-temperature diesel engine combustion," Fuel, vol. 112, pp. 459–465, 2013.